Acta Poloniae Pharmaceutica – Drug Research, Vol. 71 No. 3 pp. 451–462, 2014 ISSN 0001-6837
Polish Pharmaceutical Society

IMPROVED PHYSICOCHEMICAL CHARACTERISTICS OF ARTEMISININ USING SUCCINIC ACID

MUHAMMAD TAYYAB ANSARI[1], HUMAYUN PERVEZ[2], MUHAMMAD TARIQ SHEHZAD[2], SYED SAEED-UL-HASSAN[3], ZAHID MEHMOOD[1], SYED NISAR HUSSAIN SHAH[1], MUHAMMAD TAHIR RAZI[1] and GHULAM MURTAZA[4]*

[1]Department of Pharmacy, [2]Department of Chemistry, Bahauddin Zakariya University, Multan, Pakistan
[3]University College of Pharmacy, University of the Punjab, Lahore, Pakistan
[d]Department of Pharmaceutical Sciences, COMSATS Institute of Information Technology, Abbottabad, Pakistan

Abstract: Artemisinin (ARMN) is a potent antimalarial drug, which is effective against multidrug resistant strains of *Plasmodium falciparum* and produces rapid recovery even in patients with cerebral malaria. Being poorly soluble in water, artemisinin is incompletely absorbed after oral intake due to poor dissolution characteristics in the intestinal fluids. To enhance these properties, solid dispersions of artemisinin with succinic acid (SUC) were prepared using drug-carrier ratios 1 : 1, 1 : 4, 1 : 6, 1 : 8 and 1 : 10 by solvent evaporation and freeze drying methods. These solid dispersions were characterized by differential scanning calorimetery (DSC), Fourier transform infrared spectroscopy (FTIR), x-ray diffraction patterns (XRD), phase solubility and dissolution kinetics evaluated by applying zero order, first order, Higuchi, and Korsmeyer-Peppas models. Physical mixtures produced significantly higher aqueous solubility and rate of dissolution as compared to artemisinin alone. The dissolution profiles of all formulations followed Higuchi model and exhibited diffusion-controlled release of drug. Solvent evaporation method (SLVPs) exhibited improved solubility and freeze dried solid dispersions (FDSDs) produced highest solubility but stability constant was opposite. ARMN and SUC both were found completely crystalline as shown by their XRD patterns. Physical mixtures (PMs) showed reduced intensity in their XRD patterns while solid dispersions by SLVPs exhibited twice reduced intensity and much displaced angles, whereas FDSDs showed synergistic effects in some of ARMN and SUC peaks. DSC thermograms of FDSDs at drug-carrier ratios 1 : 1–1 : 4 showed lower melting temperature and enthalpy change (ΔH) values than respective SLVPs, whereas at higher ratios, a reverse was true. SLVPs showed displaced methyl stretching bands at lower drug-carrier ratios and exhibited O-H stretching characteristic bands of SUC at higher drug-carrier ratios. In addition, carbonyl group and C-O stretching vibrations characteristic of SUC (1307 cm^{-1}) appeared prominently compared to PMs, whereas C-O stretching characteristic bands of ARMN disappeared at higher ratios. FDSDs exhibited distinct nature of bonding compared to respective SLVPs and PMs.

Keywords: artemisinin, solubility, dissolution, solid dispersions, Korsmeyer-Peppas model

Artemisinin (qinghao, ARMN) is a naturally occurring stage specific compound with impressive blood schizonticidal and gametocytocidal activity (1–3), derived from aerial parts of plant *Artemisia annua*, causing a rapid arrest and effective treatment against drug-resistant *Plasmodium falciparum* strains within the nanomolar range (4) during malaria, which still is the most prevalent and most devastating disease in the tropics. Late stage ring parasites and trophozoites are more susceptible to artemisinin than schizonts or small rings. Unlike other antimicrobial agents, they do not possess nitrogen containing heterocyclic rings, instead, they have sesquiterpene trioxane lactone containing a peroxide bridge, which is responsible for killing intraerythrozoites. At present, ARMN holds importance in the current antimalarial campaign, as the continuous infestation and spread of resistance to antimalarial drugs among parasites is posing a serious threat of an increase in mortality rate. Numerous solid dispersion systems have been demonstrated in the pharmaceutical literature to improve the solubility and dissolution properties of poorly water soluble drugs (5–8).

Succinic acid (SUC) is a safe neutraceutical, which has been used to enhance the solubility of

* Corresponding author: e-mail: gmdogar356@gmail.com; mobile: +92-314-2082826; fax: +92-992-383441

various pharmaceuticals like rofecoxib (9), acetaminophen and theophylline (10, 11), nordazepam (12), ibuprofen (13) and griseofulvin (14). SUC has been used as an excipient for the enhanced colon-specific drug delivery (15). In addition, SUC provided the fastest rate of release in the colonic fluid compared to citric, tartaric or malic acid (16). Artemisinin solid dispersions have been studied with polyvinylpyrrolidone (17, 18), nicotinamide (19), Eudragit (20), hydroxypropylmethylcellulose, polyethyleneglycol 6000 (21), artemether with polyvinylpyrrolidone (22) and dihydroartemisinin with polyvinylpyrrolidone (23). To our knowledge, there is no report available about investigation of ARMN-SUC solid dispersions at the moment.

To find the release mechanism by dissolution studies, various models like zero-order, first order, Higuchi's and Korsmeyer-Peppas equations (24, 25) were applied to dissolution data. In zero order, the drug release is independent of its concentration (26). A first order drug release depends on drug concentration (27). The Higuchi model indicates Fickian drug release from a matrix (28). In Korsmeyer-Peppas model (29), the release exponent (n) was calculated from this model. The n = 1 indicates a release rate independent of time corresponding to zero order or case II transport, n = 0.5 stands for Fickian diffusion and n > 1 shows a super case II transport (30, 31).

Because of poor water-solubility and dissolution rate nature of artemisinin, the main objective of this work was to improve its solubility and release kinetics using different models *via* preparing solid dispersions by solvent evaporation and freeze drying methods.

MATERIALS AND METHODS

Materials

Artemisinin (Alchem, New Delhi, India), methanol (Sigma-Aldrich, Germany), succinic acid (Merck, Germany), sodium hydroxide (Merck, Germany), potassium bromide (FTIR grade, Fisher Chemicals, USA), acetone (Merck, Germany), starch (Rafhan Maize, Pakistan), lactose (DMV International, The Netherlands), magnesium stearate (Royal Tiger Products, Taiwan). Demineralized water was used for the dilution of various samples and also as the dissolution media.

Artemisinin assay

ARMN concentration measurements were carried out by following the method described previously (32), after appropriate dilution with demineralized water, adding 0.2% sodium hydroxide and heating at 40°C for 30 min. The concentration of ARMN was determined at 290 nm with a UV spectrophotometer (JENWAY, 6405 UV/ VIS, UK).

Preparation of physical mixtures (PMs)

Physical mixtures of ARMN and SUC were prepared at drug-carrier ratios 1 : 1, 1 : 4, 1 : 6, 1 : 8 and 1 : 10, respectively, by soft grinding to complete mixture with the glass pestle and mortar, afterwards, passed through the sieve (US 180 µm) and transferred to desiccators at 25°C under P_2O_5 till further use.

Preparation of solid dispersions by solvent evaporation method (SLVPs)

SLVPs were prepared using ARMN and SUC at 1 : 1, 1 : 4, 1 : 6, 1 : 8 and 1 : 10 weight ratios, respectively, by dissolving the drug and SUC in 100 mL of methanol. This solution was shaken on orbit shaker for 4–5 h at 150 rpm (25°C). Methanol was removed in rotary evaporator. These solid dispersions were pulverized, passed through 180 µm (US) mesh sieve and were transferred into colored glass bottles and stored in desiccators under the same set of conditions as that of physical mixtures till further analysis.

Preparation of freeze dried solid dispersions (FDSDs)

FDSDs were prepared using drug and carrier according to the same ratios as in SLVPs at 1 : 1, 1 : 4, 1 : 6, 1 : 8 and 1 : 10 weight ratios by dissolving ARMN and SUC in 100 mL of methanol. This solution was shaken on orbit shaker for 4–5 h at 150 rpm (25°C). Methanol was removed and 20 mL of demineralized water was added and shaken for 30 min. Afterwards, this solution was frozen at –70°C in electronic deep freezer and dried in lyophilizer. Freeze dried solid dispersions pulverized through 180 µm mesh sieve, were transferred in amber glass bottles and stored in desiccators containing P_2O_5 till further analysis.

X-ray diffraction (XRD) studies

X-ray powder diffraction of ARMN, SUC, their PMs, SLVPs and FDSDs were performed using a Siemens D500 apparatus. Measurement conditions included target CuK_α, voltage 40 KV and current 30 mA. The XRD system consisted of diverging, receiving, receiving and anti-scattering slits at angle of 1°, 1°, 1° and 0.15°, respectively. Jade 6.0 program (Materials Delta Inc. USA) was used for data processing. Patterns were obtained using a step width of 0.04° 2θ between 5 and 50°C.

Fourier transform infrared spectrophotometric (FTIR) analysis

Fourier-transform infrared (FTIR) spectra were obtained on a Shimadzu-8400S (Japan) apparatus, using the KBr disc method (0.5–1% of sample in 200 mg KBr disc) on cold press adjunct. The scanning was run at 450–4000 cm^{-1} with resolution range 1 cm^{-1}. Calibration of the instrument was performed periodically before taking spectra.

Differential scanning calorimetric (DSC) analysis

Differential scanning calorimetric (DSC) analyses of PMs, SLVPs and FDSDs were performed using Setaram 131 instrumentation. The samples were heated at the rate of 10°C/min from 40 to 290°C under dry nitrogen gas purge. Cell constants were calibrated with indium. All measurements were conducted in sealed non-hermetic aluminum pans. Typical sample weight was 5–10 mg.

Phase solubility studies

For phase solubility studies, excess quantity of each sample was taken in a 25 mL vial containing 10 mL of demineralized water. It was then placed in shaking incubator at 37 ± 1°C at 100 rpm for five days. Samples were centrifuged at 6000 rpm for 15 min and withdrawn with a syringe equipped with a 0.40 µm syringe filter. All samples were diluted to a proper concentration range and assayed for ARMN. A control experiment was also performed with pure ARMN to confirm any degradation in all used solvents. All samples were analyzed in triplicate. The apparent stability constants (K_s) of the solid dispersions were calculated from the slope of the phase solubility diagrams according to the following equation (24):

$$K_s = \frac{\text{Slope}}{S_o\ (1 - \text{slope})}$$

where S_o was the equilibrium solubility of ARMN at 37°C in the absence of SUC.

Dissolution studies

Drug release was measured using dissolution apparatus (Tablet dissolution tester GDT-7TV3, Galvano Scientific, Pakistan) at 37°C and 100 rpm, the paddle apparatus (consisting of six recipients) for high volume by using demineralized water as dissolution medium instead of a buffer (32). At predetermined time intervals (5, 15, 30, 60, 90, 120, and 180 min), 5 mL of sample were taken and replaced with the same volume of fresh solvent. Samples were assayed according to analytical procedure of AEMN described as above.

Release kinetic analysis

The release data were evaluated by zero-order, first-order, Higuchi, and Korsmeyer-Peppas models. The best model was selected based on the R^2 value.

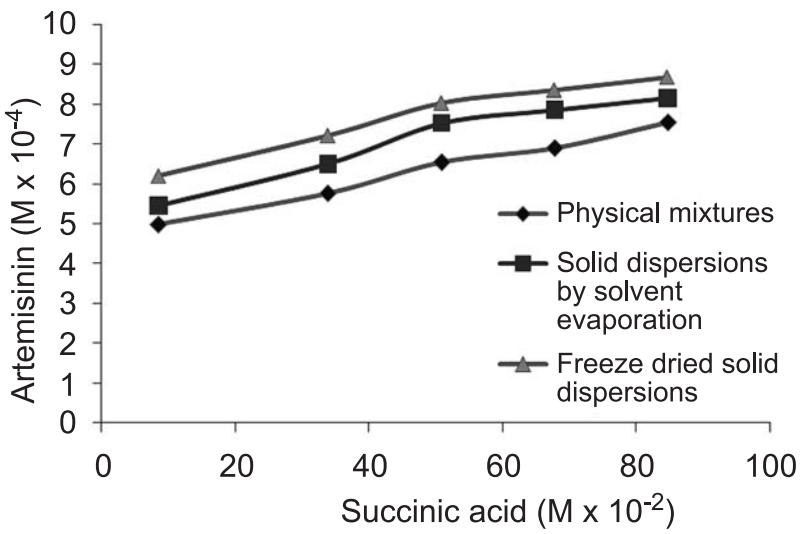

Figure 1. Phase solubility of artemisinin in physical mixtures, solvent evaporated solid dispersions (SLVPs) and freeze dried solid dispersions (FDSDs).

Table 1. Phase solubility, relative dissolution rate (RDR) and DSC results of ARMN, PMs, SLVPs and FDSDs

ARMN : SUC ratios		ΔH (J/g)	Melting onset (°C)	Peak temperature (°C)	RDR at different times (min)						Solubility ($M \times 10^{-4}$)
					5	15	30	60	90	180	
ARMN	–	44.15	149.11	151.03	–	–	–	–	–	–	0.036
PM	1 : 1	28.2	140.7	144.02	3.05	19.3	8.89	6.73	4.89	3.05	4.991
SLVP	1 : 1	19.82	139.3	142.9	3.22	20	10.1	7.4	5.78	3.54	5.435
FDSD	1 : 1	27.25	140.1	144.53	3.89	22.6	10.2	7.88	6.17	3.8	6.189
PM	1 : 4	7.414	140.4	143.24	3.39	20.9	8.99	6.78	5.09	3.24	5.766
SLVP	1 : 4	5.168	138.6	141.64	3.22	21.3	10.7	7.62	5.96	3.89	6.494
FDSD	1 : 4	3.506	139.9	142.63	4.06	23.2	11.3	8.04	6.25	3.92	7.207
PM	1 : 6	27.27	180.7	183.65	3.39	20.6	8.79	6.93	5.28	3.4	6.543
SLVP	1 : 6	41.41	182.2	184.36	4.57	24.6	11.5	7.88	6.35	4.04	7.514
FDSD	1 : 6	32.18	180.3	183.31	4.57	26	10.4	7.47	6.67	4.16	8.031
PM	1 : 8	41.18	182.2	184.74	3.89	24.6	9.79	7.31	5.42	3.48	6.895
SLVP	1 : 8	19.68	182.8	184.66	4.74	24.3	12.7	8.76	7.02	4.38	7.847
FDSD	1 : 8	28.42	182.5	184.64	4.74	30.2	12.1	8.15	6.25	4.02	8.356
PM	1 : 10	32.81	183.9	185.73	3.89	24	10.3	7.68	5.6	3.64	7.537
SLVP	1 : 10	23.19	185.3	187.16	5.08	26	11.5	8.19	6.7	4.18	8.151
FDSD	1 : 10	34.4	184.3	186.22	5.59	29	10.8	8.05	6.78	4.3	8.681

RESULTS AND DISCUSSION

Phase solubility studies

The phase solubility diagram was drawn between molar concentrations of ARMN *versus* SUC as shown in Figure 1. Solubility of ARMN was calculated as a function of SUC concentration in demineralized water. It was noted that the solubility of ARMN was enhanced with the increase in SUC concentration. Aqueous solubility of pure ARMN was found to be 0.036×10^{-6} M. Solubility of physical mixtures was found to be 7.53×10^{-4} M at 84.6×10^{-2} M of SUC concentration, whereas solubility enhancement in case of SLVPs was found to be 8.15×10^{-4} M. FDSDs exhibited more solubility than either PMs or SLVPs. Phase solubility of FDSDs at SUC concentration (84.6×10^{-2} M) was 8.68×10^{-4} M. Calculations of stability constant values for PMs, SLVPs and FDSDs yielded 12.1×10^{-2} M, 9.5×10^{-2} M and 9.3×10^{-2} M, respectively (Fig. 1 and Table 1).

Solubility of the active pharmaceutical ingredient is one of the important factors taken into consideration while developing its dosage form. Class-II drugs of BCS need improvement of their solubility to optimize their bioavailability. Phase solubility of pure ARMN and its solid dispersions were measured in demineralized water at 37°C (Table 1). SUC acid is known as a neutraceutical agent and as an excipient (9, 10–15). Keeping in mind this ability of SUC, it was applied for artemisinin. Physical mixtures produced substantial increase in the phase solubility compared to pure ARMN. They exhibited a linear increase in phase solubility of ARMN with increased SUC content. SLVPs produced further increase in solubility, i.e., 1.47–2.21 folds compared to respective PMs, that is due to interaction among drug and carrier as well as the solubilizing effect of SUC. This increase in solubility is comparable to itraconazole (33). FDSDs showed the highest solubility compared to corresponding SLVPs and PMs, respectively, while stability constant values were opposite in order. This is in accordance with respective dissolution profile discussed in previous section. Freeze drying method was found most effective for enhancing drug solubility perhaps due to an increase in surface area and the surface free energy (34–36). The slopes were lower than one in all PMs, SLVPs and FDSDs that indicate phase solubility profile was typical A_L type, which signifies that ARMN and SUC combined in 1 : 1 molar ratio similarly to diazepam (37). Our results are different from fluoxetine HCl in which SUC combined in 2 : 1 ratio, which resulted in double equilibrium solubility (38) and also different from solid dispersions of ARMN with nicotinamide, in which solubility and stability constant were the highest in FDSDs followed by SLVPs and PMs, respectively (19). Lower stability in FDSDs compared to SLVPs may be due different type of bonding reflected by our FTIR results. The high aqueous solubility of solid dispersions is attributed to high solubilizing effect of SUC similar to parabens (39). These data are consistent

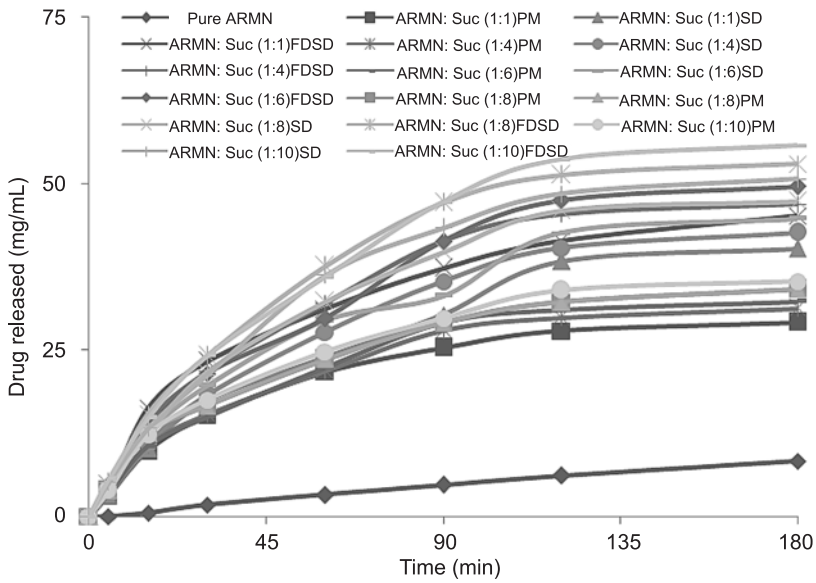

Figure 2. Dissolution curves for various formulations (ARMN – artemisinin, Suc – succinic acid)

with our XRD data, where degree of crystallinity in ARMN was reduced with enhanced SUC contents.

Dissolution profile

Physical mixtures exhibited 3.51–4.25 times higher dissolution rate than ARMN alone in demineralized water (Fig. 2.). Dissolution rate of physical mixtures increased with the rise of SUC content. SLVPs exhibited higher rate of dissolution (37.82–40.71%) than respective PMs. They exhibited 4.84 (1 : 1), 5.13 (1 : 4), 5.38 (1 : 6), 5.70 (1 :8) and 5.99 (1 : 10) times higher dissolution rate than ARMN alone, respectively. They also showed maximum dissolution rate at 1 : 10 ratio similar to corresponding PMs (Fig. 2). FDSDs exhibited the highest release rate at all ratios compared to corresponding PMs (52%) and SLVPs (12%). They showed gradual increase in dissolution rate with rise in SUC amount from 1 : 1–1 : 10 ratios, i.e., 5.44, 5.65, 5.97, 6.47, 6.60 times higher dissolution rate than ARMN alone, respectively (Fig. 2.). Relative dissolution rate (RDR) determined artemisinin solubility at different time periods in the dissolution media. The values of RDR were the highest at 15 min but it decreased with time and nearly reached to unchangeable rate after 180 min.

Dissolution rate of ARMN was increased as a function of SUC content in physical mixtures similarly to griseofulvin, where physical mixtures of 10% griseofulvin with 90% SUC showed increased dissolution rate compared to pure compound (14). This effect was attributed to increased microenvironmental solubilizing effect of SUC similar to urea (40). However, this effect was only of partial importance, because SLVPs and FDSDs showed enhanced dissolution rate than our PMs and revealed extremely fine crystals of ARMN. This was shown in XRD patterns of dispersed system, where intensity of peaks were reduced but identical crystalline structures of ARMN and SUC were observed.

The Higuchi model showed the lowest fitting values for all of the formulations. Pure ARMN followed the first order release signifying that dissolution rate is directly proportional to drug concentration in formulation. All the samples of physical mixtures fitted best in the Korsmeyer-Peppas model reflecting Fickian diffusion of drug from matrices. A release of ARMN from SLVPs was concentration dependent at 1 : 1–1 : 6 ratios, whereas at higher ratios the erosion of drug was proportional to the surface area and diameter of drug unit. FDSDs showed variable release depending upon drug-carri-

Table 2. Kinetic analysis of dissolution data.

Formulations	Zero order			First order	Higuchi	Korsmeyer-Peppas
	K_o	$T_{25\%}$ (min)	R^2	R^2	R^2	*n*
Pure ARMN	0.049	513.664	0.9898	0.9922	0.9865	0.900
ARMN : SUC (1: 1) PM	0.214	116.644	0.6308	0.7354	0.9608	0.444
ARMN : SUC (1 : 1) SD	0.279	89.455	0.8062	0.8988	0.9771	0.544
ARMN : SUC (1 : 1) FDSD	0.323	77.442	0.6515	0.8066	0.9684	0.448
ARMN : SUC (1 : 4) PM	0.229	109.154	0.6569	0.7653	0.9654	0.455
ARMN : SUC (1 : 4) SD	0.303	82.575	0.7742	0.8881	0.9723	0.526
ARMN : SUC (1 : 4) FDSD	0.342	73.040	0.7101	0.8628	0.9662	0.487
ARMN : SUC (1 : 6) PM	0.237	105.672	0.6836	0.7909	0.9656	0.471
ARMN : SUC (1 : 6) SD	0.313	79.783	0.7619	0.8809	0.9804	0.509
ARMN : SUC (1 : 6) FDSD	0.352	71.086	0.7774	0.9084	0.9739	0.526
ARMN : SUC (1 : 8) PM	0.247	101.175	0.6502	0.7681	0.9712	0.447
ARMN : SUC (1 : 8) SD	0.342	73.146	0.7363	0.8803	0.9708	0.501
ARMN : SUC (1 : 8) FDSD	0.388	64.393	0.7056	0.8839	0.9627	0.487
ARMN : SUC (1 : 10) PM	0.257	97.336	0.6602	0.7817	0.9705	0.453
ARMN : SUC (1 : 10) SD	0.366	68.225	0.7368	0.8922	0.9664	0.505
ARMN : SUC (1 : 10) FDSD	0.400	62.537	0.7582	0.9189	0.9729	0.514

er ratios, i.e., drug release was concentration dependent at 1 : 1 ratio, it transport was anomalous at 1 : 4 ratio whereas the erosion of drug was related to surface area and diameter of drug unit at 1 : 8 and 1 : 10 ratios.

Release kinetics analysis

The percent release data were fitted to several release models including zero-order, first-order, Higuchi, and Korsmeyer-Peppas models. On the basis of the highest coefficient of determination (R^2), kinetic analysis elaborates that the best fit model for dissolution data of all formulations is Higuchi's, showing the diffusion dependent release of drug from these formulations (Table 2). The role of diffusion in the release of drug from these formulations is further supported by the value of *n* obtained from the curve of Korsmeyer-Peppas model. The *n*-values are in the range of 0.444–0.544 indicating the involvement of Fickian diffusion in the release of drug from all formulations. Moreover, the value of drug release rate constant (K_0) obtained from zero order model shows that there is accelerated release of drug from formulations with the increase in concentration of SUC irrespective of technique employed for solubility enhancement, that's why ARMN : SUC (1 : 10) showed the highest rate of drug release and the rate of drug release was the slowest from ARMN : SUC (1 : 1). Dissolution curves for various formulations are shown in Figure 1, which shows that the most accelerated release of drug occurred from formulation ARMN : SUC (1 : 10) FDSD. Additionally, formulations prepared through FDSD exhibited the fastest release of drug followed by SD and then PM, thus, the methods used for formulation development can be organized (on the basis of drug release enhancing effect) as follows: FDSD > SD > PM. These results are further supported by the values of $T_{25\%}$.

Fourier transform infrared spectral studies (FTIR)

FTIR spectra of pure ARMN showed Fermi resonance of the symmetric CH_3 stretching with overtones of the methyl bending modes at 2963 cm^{-1}, C=O stretching at 1736 cm^{-1}, C-O-O-C bending (endoperoxide group) at 1123 cm^{-1}, C-O stretching at 1011 cm^{-1}, while SUC specifically produced O-H stretching at 2986 cm^{-1}, C=O stretching at 1701 cm^{-1} and C-O stretching at 1307 cm^{-1}, respectively.

FTIR spectra of physical mixtures showed shifting in O-H stretching vibrations of SUC i.e., 2961–2974 cm^{-1}, displaced carbonyl (C=O) stretching (1705–1728 cm^{-1}), slight displacement in endoperoxide bridge (C-O-O-C) stretching at 1118–1124 cm^{-1}. Stretching vibrations of C-O group representative of SUC at 1307 cm^{-1} showed slightly displaced peaks at 1310–1314 cm^{-1} while peak of C-O stretching representative of ARMN appeared only in 1 : 1 ratio at 1001 cm^{-1} and disappeared in all corresponding higher physical mixtures.

SLVPs produced O-H stretching vibrations closer to SUC (2963–2978 cm^{-1}), displaced C=O stretching (1703–1720 cm^{-1}), slight shifting in endoperoxide bridge (C-O-O-C) stretching (1116–1124 cm^{-1}) modes. Stretching vibrations of C-O group representative of SUC at 1307 cm^{-1} showed displaced peaks at 1306–1315 cm^{-1}, whereas peak of C-O stretching representing ARMN appeared only in 1 : 1 and 1 : 4 ratios at 1005 cm^{-1} and at 1008 cm^{-1}, respectively, while it disappeared in remaining ratios at higher SLVP mixtures.

FDSDs showed O-H stretching vibrations closer to SUC (2964–2982 cm^{-1}), more displaced C=O stretching (1697–1700 cm^{-1}) and slight shifting in endoperoxide bridge (C-O-O-C) stretching (1116–1126 cm^{-1}) modes. Stretching vibrations of C-O group, representative of SUC at 1307 cm^{-1}, showed displaced peaks at 1300–1311 cm^{-1} while peak of C-O stretching representative of ARMN appeared only in 1 : 1 and 1 : 4 ratios at 997 cm^{-1} and at 1002 cm^{-1}, respectively, while it disappeared in rest of the samples (Figs. not shown).

Physical mixtures revealed blue shifting in carbonyl stretching vibrations and C-O stretching peak characteristic of SUC (1307 cm^{-1}) appeared with slight red shifting and blue to red shifting in CH_3 stretching, indicating weak bonding interactions. SLVPs showed more displaced CH_3 stretching at lower ratios and exhibited O-H stretching characteristic of SUC at higher drug-carrier ratios. In addition, by increasing SUC content, carbonyl stretching frequency of SLVPs moved toward SUC. Furthermore, the C-O stretching vibrations characteristic of SUC (1307 cm^{-1}) appeared more distinct compared to PMs, while C-O stretching vibrations characteristic of ARMN (1011 cm^{-1}) disappeared at higher ratios (1 : 6–1 : 10). All this indicate enhanced interactions among ARMN and SUC in SLVPs. FDSDs, contrarily, showed red shifting in O-H stretching of succinic acid (not in PMs and SLVPs) and carbonyl group showed different kind of bonding by producing peak at lower frequency than both ARMN and SUC. In addition, they produced blue shifting in C-O stretching vibrations representative of SUC. Furthermore, C-O stretching vibrations representing ARMN showed higher blue shifting at lower ratios and disappeared at higher

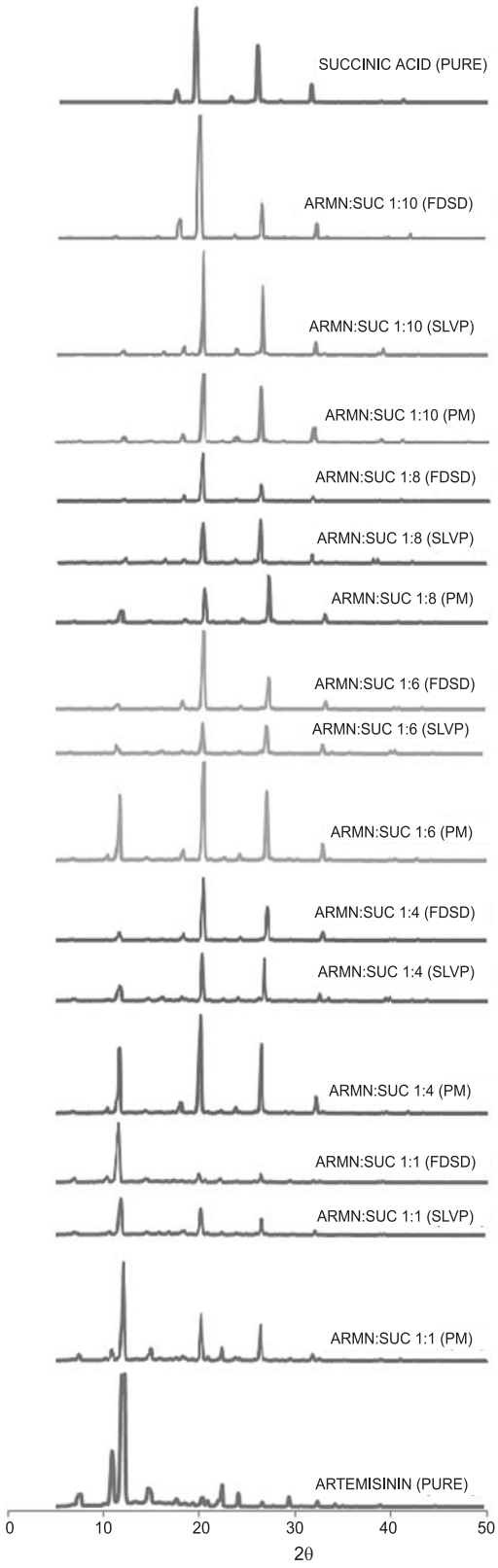

Figure 3. XRD spectra of artemisinin ARMN), succinic acid (SUC) and various preparations of artemisinin and succinic acid at drug-carrier ratios 1 : 1, 1 : 4, 1 : 6, 1 : 8 and 1 : 10

ratios (1 : 6–1 : 10). All this indicate that bonding interactions between carbonyl group of ARMN and hydroxyl group of SUC in FDSDs were of different nature compared to SLVPs and PMs, respectively. In our SLVPs and FDSDs, carbonyl group fitted stereochemically, because it finds its best position between 1720–1680 cm^{-1} (41). Furthermore, a disappearance of carbonyl stretching peak characteristic of ARMN and an appearance of carbonyl stretching peak representative of SUC at higher drug-carrier ratios also verified interaction between ARMN and SUC. Our samples at higher drug-carrier ratios showed a weak band of O-H group, which is part of the carboxyl group of SUC, similarly as reported previously (41). Displacement of stretching vibrations of C-O group (1011 cm^{-1}) representing ARMN was in the order: FDSDs > SLVPs > PMs, respectively. This peak disappeared at higher ratios correspondingly, which indicates that this group has strongly interacted with SUC, similarly to the hydrogen bonding imparted by nicotinamide with indomethacin (42) due to increased wetting ability of ARMN and solubilizing effect of the SUC. In addition, peak broadening in FTIR spectra were observed with an increase inSUC content for all PMs, SLVPs and FDSD, analogous to the carbamazepine (43). Band shifting at various functional groups, disappearance of C-O band and peak broadening are strong manifestations of interactions among ARMN and SUC. All preparations showed non-significant displacement in O-O stretching vibrations as well as stretching vibrations of endoperoxide bridge (C-O-O-C) that confirms the presence of antimalarial activity.

X-ray diffraction analysis

ARMN was observed as complete crystalline compound and XRD patterns produced strong diffraction peaks at 2θ of 10.96°, 12.20°, 14.76°, 20.44°, 22.40° and 24.12°. SUC also produced strong crystalline peaks in its XRD patterns at 2θ angle 20.12°, 26.24° and 31.68°, respectively (Fig. 3).

In physical mixtures of ARMN-SUC, a peak characteristic of ARMN at angle 2θ of 10.92° was displaced to 11.04° and showed decreased intensity with rise of SUC content. Similar behavior was exhibited by another peak of ARMN at angle 2θ of 12.20°. Characteristic peaks of SUC at angle 2θ of 20.12° was displaced from 20.08 to 20.24° and intensity at this angle increased with enhanced SUC concentration. Similarly, another characteristic peak of SUC at 2θ of 31.68° showed a displaced angle from 31.64 to 31.72° and gradual decrease in inten-

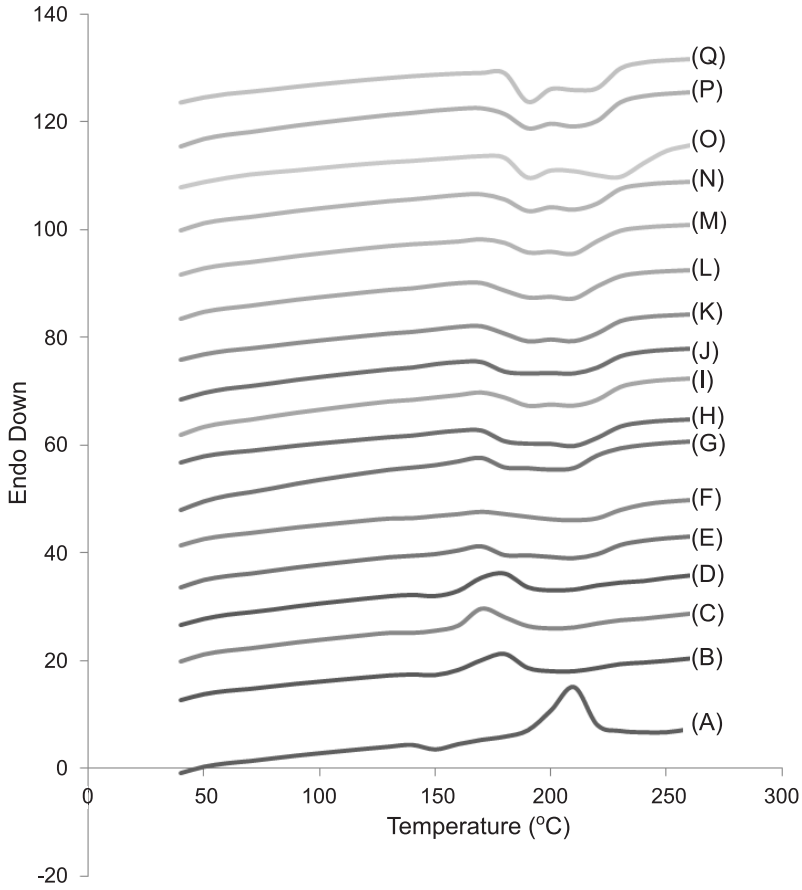

Figure 4. DSC thermograms of artemisinin (A), PMs of ARMN-SUC at 1 : 1 ratio (B), SLVPs at 1 : 1 ratio (C), FDSDs at 1 : 1 ratio (D), PMs at 1 : 4 ratio (E), SLVPs at 1 : 4 ratio (F), FDSDs at 1 : 4 ratio (G), PMs at 1 : 6 ratio (H) , SLVPs at 1 : 6 ratio (I), FDSDs at 1 : 6 ratio (J), PMs at 1 : 8 ratio (K), SLVPs at 1 : 8 ratio (L), FDSDs at 1 : 8 ratio (M), PMs at 1 : 10 ratio (N), SLVPs at 1 : 10 ratio (O), FDSDs at 1 : 10 ratio (P), succinic acid (Q)

sity with an increase in SUC content, as shown in Figure 3.

In SLVPs, a peak characteristic of pure ARMN at angle 2θ of 10.92° disappeared at all concentrations. Another characteristic peak at angle of 12.12° produced less than a half intensity compared to respective physical mixtures. Peaks at 14.76° were displaced to 15.28° having very low intensity at 1 : 4–1 : 6 ratios, while they disappeared at 1 : 6–1 : 10 ratios. Characteristic peaks of SUC at 2θ of 20.40° and at 2θ of 26.24° revealed intensity less than a half at 1 : 1–1 : 8 ratios but at 1 : 10 ratio this was almost doubled in relation to corresponding PMs. In addition, 2θ of 31.68° showed more displaced angle 2θ of 31.68–31.96° and about a half intensity than respective PMs.

FDSDs also produced no peak at 2θ of 10.92°. A peak at 12.16° exhibited more intensity than corresponding SLVPs at 1 : 1–1 : 8 ratios but showed lower intensity at 1 : 10 ratio. Another peak at 2θ of 14.88° was present only at 1 : 1 ratio, while it was absent at higher ratios. Peculiar feature of FDSDs was that a peak at 2θ of 18.32° appeared with lower intensity at 1 : 1–1 : 8 ratios than both its ingredients but at 1 : 10 ratio its intensity was more than both ARMN and SUC. Similar behavior was noted at 2θ of 20.28° but ratio was 1 : 8 and 1 : 10. Furthermore, angle 2θ of 31.68° produced a shifted angle from 31.68 to 31.88° with the lowest intensity compared to respective SLVPs and PMs.

ARMS as well as SUC was found to be completely crystalline in its XRD patterns. X-ray diffraction studies of various preparations showed altered patterns, which signify bonding interactions among ARMN and SUC depending upon extent of alterations. Physical mixed samples showed dis-

placed angles and decreased intensities that indicate bonding interactions, which agrees with solubility, dissolution and FTIR findings. Peak characteristic of ARMN at 10.92° disappeared in all SLVPs and FDSDs compared to the presence in PMs, indicating comparatively stronger interactions. Another characteristic peak at 12.12° in SLVPs showed less than half intensity and peak at 15.28° disappeared at higher drug-carrier ratio verifying these interactions. SLVPs showed the lowest peak intensities compared to respective FDSDs and PMs at 12.24, 20.12, 31.68° and most displaced angles at 14.76° that indicate somewhat stronger interactions in ARMN area and weaker interactions of SUC area. The increased solubility and dissolution rate of ARMN with SUC in SLVPs was attributed to glass dispersions so as the reason in the dissolution enhancement of rofecoxib by employing citric acid (9).

FDSDs showed variable results especially at higher drug-carrier ratios, i.e., the lowest intensity in 1 : 10 ratio at 12.24° while at other ratios it was higher than PMs; similarly, it had the highest peak intensity at 31.68° even more than SUC itself, which is characteristic of synergy. Such behavior was also noted at 20.12° when FDSDs produced the highest intensity even more than ARMN and SUC at 1 : 6–1 : 10 ratios. This synergistic effect verifies different type of bonding in FDSDs compared to SLVPs and PMs at higher ratios agrees with our FTIR spectra. In addition, FDSDs showed higher intensity than corresponding SLVPs in 1 : 1–1 : 8 ratios at 31.68° indicating that SUC made stronger bonding interactions compared to SLVPs, which agrees with our solubility and dissolution profile. This behavior was similar to flurbiprofen and ARMN with nicotinamide in solid dispersions, respectively (19, 44, 45), at low drug content ratio, because at higher carrier content solid dispersion behavior turned more towards the SUC due to the possible fine dispersion of ARMN in the carrier content. Hence, rearranged angles, synergistic effect and disappearance of some crystalline peaks verify the drug-carrier interactions.

Differential scanning calorimetry

ARMN showed melting onset temperature at 149.11°C and peak temperature at 151.03°C while ΔH value was 44.15 J/g. SUC produced ΔH value of 79.84 J/g, melting onset melting temperature of 186.88°C having peak temperature at 188.30°C. Enthalpy changes (ΔH), peak temperature and melting onset melting temperatures of physical mixture, solid dispersion and freeze dried solid dispersion are given in Table 1. Physical mixtures showed two kinds of melting temperatures i.e., one near melting temperature of ARMN at drug-carrier ratio 1 : 1–1 : 4, other near melting temperature of SUC i.e., at drug-carrier ratio 1 : 6–1 : 10. Physical mixtures at 1 : 1–1 : 4 ratios showed melting onset temperature 138.6–140.7°C and peak temperature 141.64–144.53°C whereas at 1 : 6–1 : 10 ratios melting onset temperature 180.7–183.9°C and peak temperature 183.65–185.73°C. All samples showed ΔH values lower than that of ARMN.

SLVPs exhibited higher melting temperatures than respective PMs, i.e., melting onset temperatures at 182.2–185.3°C and peak temperature at 184.36–187.16°C for 1 : 6–1 : 10 ratios and ΔH values 19.68–41.41 J/g, respectively. FDSDs showed lower melting temperatures than corresponding SLVPs, i.e., melting onset temperatures 180.31–184.30°C, while peak temperatures 183.31–186.22°C and enthalpy change values 28.42–34.4 J/g, respectively (Fig. 4).

Differential scanning thermograms revealed decreased melting onset and peak temperatures of ARMN at 1 : 1–1 : 4 ratios, while at 1 : 6–1 : 10 ratios melting onset and peak temperatures were near those of SUC but lower than those of SUC in all preparations of PMs, SLVPs and FDSDs. SLVPs exhibited the lowest melting temperatures followed by FDSDs and PMs, respectively, at 1 : 1–1 : 4 ratios, whereas FDSDs revealed lower melting temperatures than corresponding SLVPs at 1 : 6–1 : 10 ratios. It indicates the presence of stronger bonding interactions at 1 : 6–1 : 10 ratios that coincide with XRD patterns, FTIR spectra and relative dissolution rate (RDR).

Similarly, enthalpy changes (ΔH) of all prepared samples of PMs, SLVPs and FDSDs were lower than those of ARMN and SUC. Enthalpy change (ΔH) values for all prepared samples of PMs, SLVPs and FDSDs at ratio 1 : 4 were found to be lowest than for all other samples, which indicates that thermal stability was the lowest at this ratio, while other ratios showed moderate thermal stability values but lower than those for ARMN as well as SUC. It might be due to masking effect of carrier and amorphization, as well as fine dispersion of ARMN as shown from the DSC thermograms and XRD spectra. In addition, FDSDs at 1 : 8–1 : 10 ratios exhibited higher ΔH values than corresponding SLVPs, which is in agreement with XRD spectra but opposite to stability constant, that is indicative of different nature of interactions among SUC and ARMN.

Decreased enthalpy values, shifting of melting temperatures and peak broadening in DSC thermograms confirm the interaction between drug and car-

rier that is supported by decreased peak intensities, displaced angles in XRD patterns, red and blue shifting of stretching frequencies in FTIR spectra, enhanced solubility and dissolution profile.

CONCLUSION

It can be concluded from the results that ARMN solubility and dissolution rate can be enhanced by preparing its freeze dried solid dispersions using SUC as solubility enhancer.

Acknowledgments

Authors are thankful to Higher Education Commission (HEC) of Pakistan for providing funding for research project No. 2550 due to which this work was possible and Hamaz Pharmaceutical Company, Multan, Pakistan for providing facility of some instruments.

REFERENCES

1. Dutta G.P., Mohan A., Tripathi R.: J. Parasitol. 76, 849 (1990).
2. Sher M., Hussain G., Hussain M.A., Akhtar T., Akram M.R., Paracha R.N., Murtaza G.: Afr. J. Pharm. Pharmacol. 6, 2424 (2012).
3. Murtaza G., Ahmad M., Madni M.A., Asghar M.W.: Bull. Chem. Soc. Ethiop. 23, 1 (2009).
4. Khan S.A., Ahmad M., Murtaza G., Shoaib H.M., Aamir M.N., Kousar R., Rasool F., Madni A.: Latin Am. J. Pharm. 29, 1029 (2010).
5. Khan S.A., Ahmad M., Murtaza G., Aamir M.N., Kousar R., Rasool F., Zaman S.U.: Acta Pharm. Sin. 45, 772 (2010).
6. Ahmad M., Iqbal M., Akhtar N., Murtaza G., Madni M.A.: Pak. J. Zool. 42, 395 (2010).
7. FDA guideline (1987). Guidelines on General Principles of Process Validation, p. 4, US Food and Drug Administration. Maryland, USA.
8. Rasool F., Ahmad M., Khan H.M.S., Akhtar N., Murtaza G.: Acta Pol. Pharm. Drug Res. 67, 185 (2010).
9. Ahmad M., Ahmad R., Murtaza G.: Adv. Clin. Exp. Med. 20, 599 (2011).
10. Khiljee S., Ahmad M., Murtaza G., Madni M.A., Akhtar N., Akhtar M.: Pak. J. Pharm. Sci. 24, 421 (2011).
11. Khan M.I., Murtaza G., Awan S., Iqbal M., Waqas M.K.: Afr. J. Pharm. Pharmacol. 5, 143 (2011).
12. Aamir M.F., Ahmad M., Murtaza G., Khan S.A.: Latin Am. J. Pharm. 30, 318 (2011).
13. Ahmad M., Murtaza G., Akhtar N., Siddique F., Khan S.A.: Acta Pol. Pharm. Drug Res. 68, 115 (2011).
14. Chiou W.L., Niazi S.: J. Pharm. Sci. 65, 1212 (1976).
15. Nykanen P., Krogars K., Sakkinen M.: Int. J. Pharm. 184, 51 (1999).
16. Kaur K., Kim K.: Int. J. Pharm. 366, 140 (2009).
17. Ansari M.T., Haneef M., Murtaza G.: Adv. Clin. Exp. Med. 19, 745 (2010a).
18. Nijlen V.T., Brennan K., Mooter G.V.D.: Int. J. Pharm. 254, 173 (2003).
19. Ansari M.T., Pervez H., Shehzad M.T.: Pak. J. Pharm. Sci. 25, 447 (2012).
20. Hoa N.D., Long N.V.: Tap. Chi. Duoc. Hoc. 12, 17 (1999).
21. Long N.V., Hao D.N., Duong P.T.T.: Tap. Chi. Duoc. Hoc. 8, 15 (1999).
22. Ansari M.T., Karim S., Ranjha N.M.: Arch. Pharm. Res. 33, 901 (2010b).
23. Ansari M.T., Sunderland V.B.: Arch. Pharm. Res. 31, 390 (2008).
24. Costa P., Lobo J.M.S.: Eur. J. Pharm. Sci. 13, 123 (2001).
25. Philip A.K., Pathak K.: AAPS PharmSciTech 7, E1 (2006).
26. Najib N., Suleiman M.: Drug Dev. Ind. Pharm. 11, 2169 (1985).
27. Desai S.J., Sing P., Simonelli A.P.: J. Pharm. Sci. 55, 1230 (1966).
28. Higuchi T.: J. Pharm. Sci. 52, 1145 (1963).
29. Korsmeyer R.W., Gurrny R., Doelker E.M.: Int. J. Pharm. 23, 25 (1983).
30. Ritger P.L., Peppas N.A.: J. Control. Release 5, 37 (1987).
31. Siepmann J., Peppas N.A.: Adv. Drug Deliv. Rev. 48, 139 (2001).
32. Ngo T.H., Michael A., Kinget R.: Int. J. Pharm. 138, 185 (1996).
33. Zhao S.S., Zeng M.Y.: Planta Med. 3, 233 (1985).
34. Schultheiss N., Newman A.: Cryst. Growth Des. 9, 2950 (2009).
35. Onyeji C.O., Omoruyi S.I., Oladimeji F.A.: Pharmazie 62, 858 (2007).
36. Pose-Vilarnovo B., Perdomo-Lopez I., Echezarreta-Lopez M.: Eur. J. Pharm. Sci. 13, 325 (2001).
37. Betageri G.V., Makarla K.R.: Int. J. Pharm. 126, 155 (1995).
38. Rasool A.A., Hussain A.A., Dittert L.W.: J. Pharm. Sci. 80, 387 (1991).
39. Childs S.L., Chyall L.J., Dunlap J.T.: J. Am. Chem. Soc. 126, 13335 (2004).

40. Nicoli S., Zani F., Bilzi S.: Eur. J. Pharm. Biopharm. 69, 613 (2008).
41. Goldberg H., Gibaldi M., Kanig J.L.: J. Pharm. Sci. 55, 482 (1966).
42. Mitsui K., Ukaji T.: Infrared spectra of some aqueous solutions. Research Reports of Ikutoku Technical University (1977).
43. Jain A.K.: Eur. J. Pharm. Biopharm. 68, 701 (2008).
44. Sethia S., Squillante E.: Int. J. Pharm. 272, 1 (2004).
45. Varma M.M., Pandi J.K.: Drug Dev. Ind. Pharm. 31, 417 (2005).

Received: 22. 07. 2013